

Modeling Random Methyl Branching in Ethylene/ Propylene Copolymers Using Metathesis Chemistry: Synthesis and Thermal Behavior

John C. Sworen,[‡] Jason A. Smith,[‡] Kenneth B. Wagener,^{*,‡} Lisa S. Baugh,^{†,§} and Steven P. Rucker[§]

Contribution from the The George and Josephine Butler Polymer Research Laboratory, Department of Chemistry, University of Florida, Gainesville, Florida 32611-7200 and Corporate Strategic Research Laboratory, ExxonMobil Research and Engineering Company, 1545 Route 22 East, Annandale, New Jersey 08801-3059

Received June 20, 2002; E-mail: wagener@chem.ufl.edu.

Abstract: The structure of random ethylene/propylene (EP) copolymers has been modeled using step polymerization chemistry. Six ethylene/propylene model copolymers have been prepared via acyclic diene metathesis (ADMET) polymerization and characterized for primary and higher level structure using in-depth NMR, IR, DSC, WAXD, and GPC analysis. These copolymers possess 1.5, 7.1, 13.6, 25.0, 43.3, and 55.6 methyl branches per 1000 carbons. Examination of these macromolecules by IR and WAXD analysis has demonstrated the first hexagonal phase in EP copolymers containing high ethylene content (90%) without the influence of sample manipulation (temperature, pressure, or radiation). Thermal behavior studies have shown that the melting point and heat of fusion decrease as the branch content increases. Further, comparisons have been made between these random ADMET EP copolymers, random EP copolymers made by typical chain addition techniques, and precisely branched ADMET EP copolymers.

Introduction

Polyethylene is the largest volume synthetic macromolecule produced today and is the fastest growing petrochemical market in the world, with over 100 billion pounds produced in 2001.¹ Since commercial inception in the 1930s, considerable research has focused on the structure–property relationships of ethylene based polymers. The ultimate effect that branching has on the behavior of polyolefins is quite important; in fact, this topic has been examined in great detail for more than 60 years.^{2–10}

Indeed, the melting behavior and branch analysis of ethylene/ α -olefin random copolymers has garnered considerable attention due to wide-ranging perturbations in the final materials response associated with the distribution of the α -olefin within the copolymer.¹¹ The properties and performance of ethylene-based copolymers is dependent primarily on branch content and comonomer incorporation along a single chain and, most importantly, between polymer chains.¹¹ Consequently, modeling such behavior can lead to a better understanding of not only polymer processing but also the overall effect microstructural branch perturbations have on polyethylene (PE) based materials.

Until now, modeling random (statistical) branching in polyethylene has been restricted to polymers produced by chain addition chemistry using either free radical chemistry,¹² Ziegler–

[†] Previous work published as Lisa S. Boffa.

[‡] University of Florida.

[§] ExxonMobil Research and Engineering Company.

- (1) Univation Technologies – Market Information. <http://www.univation.com/markets/market.asp>.
- (2) (a) Ke, B. *J. Polym. Sci.* **1962**, *61*, 47–59. (b) Gutzler, F.; Wegner, G. *Colloid and Polym. Sci.* **1980**, *258*, 776–778.
- (3) Mirabella, F. M., Jr.; Ford, E. A. *J. Polym. Sci., Part B: Polym. Phys.* **1987**, *25*, 777–790.
- (4) Alamo, R. G.; Mandelkern, L.; Stack, G. M.; Krönke, C.; Wegner, G. *Macromolecules* **1994**, *27*, 147–156.
- (5) Alamo, R. G.; Mandelkern, L. *Macromolecules* **1989**, *22*, 1273–1277.
- (6) Wunderlich, B.; Poland, D. *J. Polym. Sci., Part A* **1963**, *1*, 357–372.
- (7) (a) Gerum, W.; Hohne, G. W. H.; Wilke, W.; Arnold, M.; Wegner, T. *Macromol. Chem. Phys.* **1996**, *197*, 1691–1712. (b) Shroff, R.; Prasad, A.; Lee, C. *J. Polym. Sci., Part B: Polym. Phys.* **1996**, *34*, 2317–2333. (c) Pieski, E. T. *Polyethylene*; Renfrew, A.; Morgan, P., Eds. Interscience Publishers: New York, 1960. (d) Ke, B. *J. Polym. Sci.* **1960**, *42*, 15–23.
- (8) (a) Kawaguchi, T.; Ito, T.; Kawai, H.; Keedy, D.; Stein, R. S. *Macromolecules* **1968**, *1*, 126–133. (b) Lambert, W. S.; Phillips, P. *J. Polymer* **1996**, *37*, 3585–3591. (c) Kim, Y.; Kim, C.; Park, J.; Kim, J.; Min, T. *J. Appl. Polym. Sci.* **1996**, *60*, 2469–2479, and references therein. (d) Gerum, W.; Hohne, G. W. H.; Wilke, W.; Arnold, M.; Wegner, T. *Macromol. Chem. Phys.* **1995**, *196*, 3797–3811.
- (9) (a) Mandelkern, L.; Glotin, M.; Benson, R. A. *Macromolecules* **1981**, *14*, 22–34. (b) Alamo, R. G.; Chan, E. K. M.; Mandelkern, L.; Voight-Martin, I. G. *Macromolecules* **1992**, *25*, 6381–6394. (c) Alamo, R. G.; Viers, B. D.; Mandelkern, L. *Macromolecules* **1993**, *26*, 5740–5747.

- (10) (a) Schumacher, M.; Lovinger, A. J.; Agarwal, P.; Wittmann, J. C.; Lotz, B. *Macromolecules* **1994**, *27*, 6956–6962. (b) Hashimoto, T.; Prud'homme, R. E.; Stein, R. S.; *J. Polym. Sci., Polym. Phys. Ed.* **1973**, *11*, 709–736.
- (11) (a) Ungar, G.; Zeng, X–b. *Chem. Rev.* **2001**, *101*, 4157–4188. (b) Bracco, S.; Comotti, A.; Simonutti, R.; Camurati, I.; Sozzani, P. *Macromolecules* **2002**, *35*, 1677–1684. (c) DesLauriers, P. J.; Rohlfing, D. C.; Hsieh, E. T. *Polymer* **2002**, *43*, 159–170. (d) Zhang, F.; Song, M.; Lü, T.; Liu, J.; He, T. *Polymer* **2002**, *43*, 1453–1460. (e) Starck, P.; Malmberg, A.; Löfgren, B. *J. Appl. Polym. Sci.* **2002**, *83*, 1140–1156. (f) Jokela, K.; Väinänen, A.; Torckeli, M.; Starck, P.; Serimaa, R.; Löfhren, B.; Seppälä, J. *J. Polym. Sci., Polym. Phys.* **2001**, *39*, 1860–1875. (g) Wright, K. J.; Lesser, A. J. *Macromolecules* **2001**, *34*, 3626–3633. (h) Pak, J.; Wunderlich, B. *Macromolecules* **2001**, *34*, 4492–4503. (i) Zhang, X–b.; Li, Z–s.; Lu, Z–y.; Sun, C–c. *J. Chem. Phys.* **2001**, *115*, 3916–3922. (j) Walter, P.; Heinemann, J.; Ebeling, H.; Mader, D.; Trinkle, S.; Rolf, M. *Organomet. Catal. Olefin Polym.* **2001**, 317–327. (k) Haigh, J. A.; Nguyen, C.; Alamo, R. G.; Mandelkern, L. *J. Therm. Anal. Calorim.* **2000**, *59*, 435–450. (l) Hadjichristidis, N.; Xenidou, M.; Iatrou, H.; Pitsikalis, M.; Poulos, Y.; Avgeropoulos, A.; Sioula, S.; Paraskeva, S.; Velis, G.; Lohse, D. J.; Schulz, D. N.; Fetters, L. J.; Wright, P. J.; Mendelson, R. A.; García-Franco, C. A.; Sun, T.; Ruff, C. *J. Macromolecules* **2000**, *33*, 2424–2436.

Natta chemistry,¹³ homogeneous metallocene,¹⁴ and/or late transition metal catalytic systems.^{15,16} Inevitably, chain transfer or chain walking occurs, causing unwanted branching, broad molecular weight distributions, and heterogeneous comonomer distribution.¹⁷ These “defects” in the polymer structure, exploited to create wider and varying material responses, can be unfavorable when attempting to synthesize ideal models for ethylene/ α -olefin copolymers. Our approach to this problem is quite different from previous studies. We have chosen step polycondensation chemistry to model PE, a methodology that precludes the random branching resulting from chain transfer reactions.

The Acyclic Diene METathesis (ADMET) reaction has been used to produce linear polyethylene via polymerization of 1,9-decadiene to polyoctenamer, followed by subsequent hydrogenation to yield what we term as ADMET PE.¹⁸ Further, ADMET has been used to create ethylene/propylene copolymers wherein the methyl branch is precisely placed along the macromolecular backbone. Previously, we reported that model EP copolymers with a precise sequence length distribution between methyl branches exhibit properties not seen in model EP copolymers produced by chain addition polymerization to date.¹⁹

In this paper, we expand our ADMET model approach by synthesizing a series of random EP materials containing varying degrees of propylene incorporation, focusing primarily on the characterization of chain structure and thermal behavior. Copolymerizing the appropriate methyl branched α,ω -diene monomer with a linear, unbranched hydrocarbon α,ω -diene, followed by subsequent exhaustive hydrogenation leads to

statistical methyl branching along the chain, where the final microstructure is controlled both by the monomers chosen and the molar ratios used during the polymerization. Herein, we report our findings for six copolymer systems with varying degrees of short-chain branching (SCB) content.

Results and Discussion

A. Polymer Synthesis and Hydrogenation. ADMET polycondensation was used as the modeling polymerization mechanism of choice because it offers control of the molecular weight distribution, branch type, and comonomer distribution in the final copolymer. Manipulation of these variables for PE has been sought for some time, since doing so provides a protocol to fine-tune the mechanical properties, morphology, and response of the final copolymer. It is our intent to define macromolecular structure/property relationships for PE copolymers using this approach.

For example, stiffness, tensile strength, processability, and softening are all properties affected by short chain branching (SCB) and short chain branch distribution (SCBD) in PE based materials.²⁰ ADMET can control the branching sequence length distribution in the microstructure of the final copolymer by allowing for total conversion of monomer(s). Because this is step polycondensation chemistry, the initial molar ratio of the two monomers is directly transferred to the final copolymer; one does not have to deal with reactivity ratios. Further, ADMET copolymerization produces a random copolymer as a result of the transmetathesis reaction of internal olefins, a phenomenon exactly analogous to transesterification which occurs in the synthesis of poly(ethylene terephthalate).

The nomenclature for the unsaturated ADMET copolymers is designed to describe the actual branch content (**PE-43.3**, 43.3 being the number of CH₃ branches/1000 total carbons measured by NMR), whereas the hydrogenated samples contain an “H” after the branch number (i.e., **PE-43.3H**). In this study, six model EP copolymers were synthesized by combining 6-methyl-1,10-undecadiene (**1**) and 1,9-decadiene (**2**) with Schrock’s molybdenum metathesis catalyst under ADMET polymerization conditions (Figure 1). Additionally, homopolymers derived from monomers **1** and **2** have been synthesized for comparison. Monomer **1** and **PE-97.4H** used in this study were synthesized following literature procedure.¹⁹ The homopolymers of 1,9-decadiene are designated **PE-OCT** and **PE-OCTH** (“polyoctenamer”).

All monomers were dried over metal, and the highest molar ratio of monomer to catalyst was employed. The chemistry proceeds smoothly to produce linear unsaturated polymers with no side reactions detectable by NMR analysis. The three copolymers containing the highest branch content (**PE-43.3**, **PE-55.6**, and homopolymer **PE-97.4**, which carries a methyl “branch” in every repeat unit) remained viscous liquids throughout the polymerization, whereas the remaining polymers solidified within 5 min of initiation. These observations are a direct reflection of the effect that methyl SCB and SCBD have on the behavior of the resulting materials.

Prior to saturation with hydrogen, the unsaturated copolymers were characterized by quantitative ¹³C NMR spectroscopy, which determined the cis:trans ratio of the double bond for all

- (12) Fawcett, E. W.; Gibson, R. Q.; Perrin, M. H.; Patton, J. G.; Williams, E. G. *Brit. Pat.* 2, 816, 883, Sept. 6, 1937 (Imperial Chemical Industries, Ltd.).
- (13) (a) Mirabella, F. M. *J. Polym. Sci., Polym. Phys.* **2001**, 39, 2800–2818. (b) Dias, M. L.; Barbi, V. V.; Pereira, R. A.; Mano, E. B. *Mater. Res. Innovat.* **2001**, 4, 82–88. (c) Ziegler, K. *Kunststoffe* **1955**, 45, 506. (d) Ziegler, K. *Belg. Pat.* 533, 326, May 5, 1955.
- (14) (a) Quijada, R.; Rojas, R.; Bazan, G.; Komon, Z. J. A.; Mauler, R. S.; Galland, G. B. *Macromolecules* **2001**, 34, 2411–2417. (b) Liu, J.; Zhang, F.; He, T. *J. Mater. Sci.* **2001**, 36, 5345–5349. (c) Zhu, F.; Fang, Y.; Chen, H.; Lin, S. *Macromolecules* **2000**, 33, 5006–5010. (d) Kravchenko, R.; Waymouth, R. M. *Macromolecules* **1998**, 31, 1–6. (e) Jüngling, S.; Koltzenburg, S.; Mühlaupt, R. *J. Polym. Sci. Polym. Chem.* **1997**, 35, 1–8. (f) Sinn, H.; Kaminsky, W. Ziegler–Natta Catalysts. *Advances in Organometallic Chemistry*; Academic Press Inc.: London, 1980; p 99–149. (g) James, D. E. *Ethylene Polymers: Encyclopedia of Polymer Science and Engineering*, 2nd ed. Wiley-Interscience: New York, 1986, p 329.
- (15) (a) Komon, Z. J. A.; Bazan, G. C. *Macromol. Rapid Commun.* **2001**, 22, 467–478. (b) Mäder, D.; Heinemann, J.; Walter, P.; Mühlaupt, R. *Macromolecules* **2000**, 33, 1254–1261. (c) Rix, F.; Brookhart, M. *J. Am. Chem. Soc.* **1995**, 117, 1137–1138. (d) Peuckert, M.; Keim, W. *Organometallics* **1983**, 2, 594–597. (e) Wilke, G. *Angew. Chem., Int. Ed. Engl.* **1988**, 27, 185–206. (f) Möhring, V. M.; Fink, G. *Angew. Chem., Int. Ed. Engl.* **1985**, 24, 1001–1003. (g) Schmidt, G. F.; Brookhart, M. *J. Am. Chem. Soc.* **1985**, 107, 1443–1444. (h) Brookhart, M.; Volpe, A. F., Jr.; Lincoln, D. M.; Horvath, I. T.; Millar, J. M. *J. Am. Chem. Soc.* **1990**, 112, 5634–5636. (i) Keim, W.; Kowaldt, F. H.; Goddard, R.; Krüger, C. *Angew. Chem., Int. Ed. Engl.* **1978**, 17, 466–467. (j) Klabunde, U.; Ittel, S. D. *J. Mol. Catal.* **1987**, 41, 123–134.
- (16) (a) Small, B. L.; Brookhart, M.; Bennett, A. M. A. *J. Am. Chem. Soc.* **1998**, 120, 4049–4050. (b) Kim, J. S.; Pawlow, J. H.; Wojcinski, L. M., II.; Murtuza, S.; Kacker, S.; Sen, A. *J. Am. Chem. Soc.* **1998**, 120, 1932–1933. (c) Johnson, L. K.; Killian, C. M.; Brookhart, M. *J. Am. Chem. Soc.* **1995**, 117, 6414–6415. (d) Johnson, L. K.; Killian, C. S.; Author, S. D.; Feldman, J.; McCord, E. F.; McLain, S. J.; Kreutzer, K. A.; Bennett, M. A.; Coughlin, E. B.; Ittel, S. D.; Parthasarathy, A.; Tempel, D. J.; Brookhart, M. S. *Intl. Pat. Appl. WO96/23010* 1996. (e) Feldman, J.; McLain, S. J.; Parthasarathy, A.; Marshall, W. J.; Calabrese, J. C.; Arthur, S. D. *Organometallics* **1997**, 16, 1514–1516. (f) Long, D. P.; Bianconi, P. A. *J. Am. Chem. Soc.* **1996**, 118, 12 453–12 454.
- (17) (a) Gates, D. P.; Svejda, S. A.; Oñate, E.; Killian, C. M.; Johnson, L. K.; White, P. S.; Brookhart, M. *Macromolecules* **2000**, 33, 2320–2334. (b) Mattice, W. L. *Macromolecules* **1983**, 16, 487–490. (c) Mattice, W. L.; Stehling, F. C. *Macromolecules* **1981**, 14, 1479. (d) Roedal, M. J. *J. Am. Chem. Soc.* **1953**, 75, 6110–6112.
- (18) O’Gara, J. E.; Wagener, K. B.; Hahn, S. F. *Makromol. Chem., Rapid Commun.* **1993**, 14, 657–662.
- (19) Smith, J. A.; Brzezinska, K. R.; Valenti, D. J.; Wagener, K. B. *Macromolecules* **2000**, 33, 3781–3794.

- (20) Sun, T.; Brant, P.; Chance, R. R.; Graessley, W. W. *Macromolecules* **2001**, 34, 6812–6820.

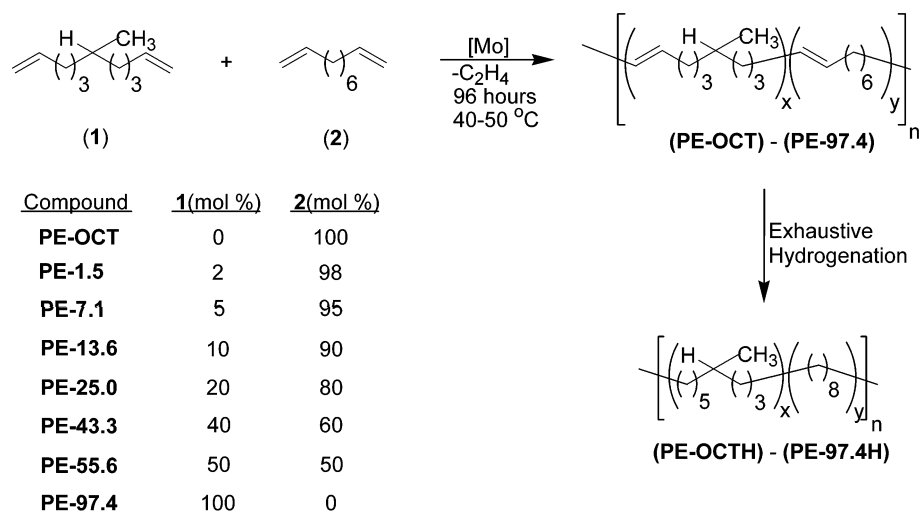


Figure 1. General Synthetic Scheme for the Synthesis of EP Model Copolymers (theoretically determined mol %).

eight polymers. When polymerizing unhindered monomers such as 1,9-decadiene Schrock's [Mo] catalyst produces polymers with a trans content greater than 90%;¹⁸ however, when the molar ratio of the "methyl" monomer **1** is increased, the trans content decreases.¹⁹ The homopolymerization of 1,9-decadiene produces a polymer with a trans fraction of 96%, a value which decreases to 85% for the copolymerization of a 50/50 molar ratio 1,9-decadiene and 6-methyl-1,10-undecadiene and 77% for the homopolymer of 6-methyl-1,10-undecadiene. This change in cis:trans ratio is due to the increased methyl branching (defect) content. Further, an increase in branch content may lead to more chain-folded gauche interactions during the materials crystallization (most likely via a chain-folding mechanism), which leads to a better understanding of the crystallization kinetics in these unsaturated materials and may permit the modeling of ethylene propylene diene monomer (EPDM) rubbers. Research is currently underway to model EPDM elastomeric materials to further substantiate this observation.

The unsaturated ADMET copolymers described above were transformed into model EP analogues by exhaustive hydrogenation using Wilkinson's catalyst. A homogeneous hydrogenation method was chosen to accommodate the insolubility of the resulting saturated polymers, thereby offering more facile purification after complete saturation of the olefin bond present in each repeat unit. Previously, Wilkinson's catalyst has been shown to successfully hydrogenate radically produced branched polybutadienes, a fact that guided our choice of hydrogenation systems.²¹ The complete hydrogenation of **PE-43.3** and **PE-55.6** was accomplished in 96 h using toluene as the solvent, whereas the copolymers **PE-OCTH** – **PE-25.0H** required a higher boiling solvent (xylene at 145 °C) to maintain homogeneous hydrogenation conditions. In both cases, full hydrogenation was achieved. The hydrogenation proceeds more efficiently with the exclusion of moisture and oxygen from the reaction vessel.

While there are several analytical techniques to monitor successful hydrogenation (¹H NMR, ¹³C NMR, bromine uptake,

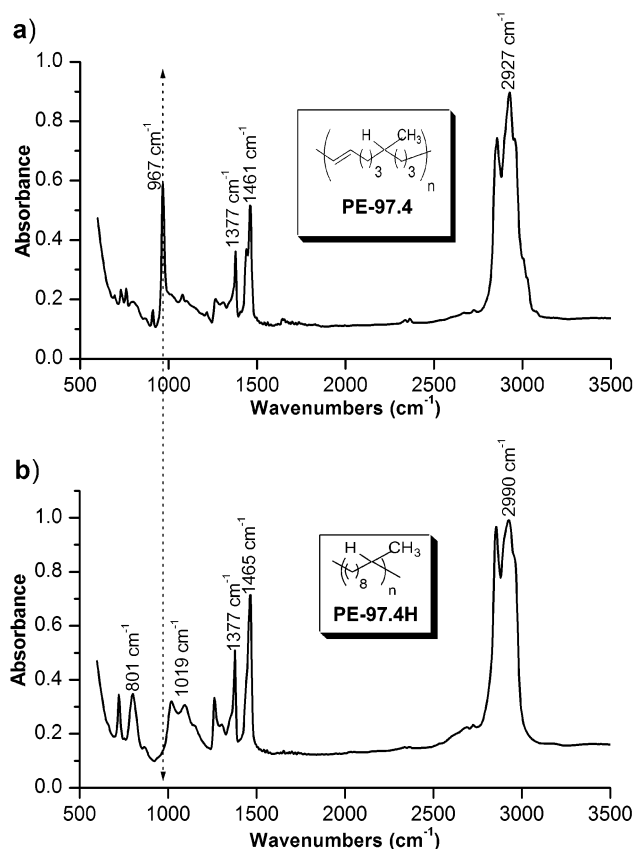


Figure 2. (a) IR of ADMET prepolymer PE-97.4 and (b) PE-97.4H.

and infrared (IR) spectroscopy), IR spectroscopy offers the most sensitive method to observe whether exhaustive saturation has occurred. Figure 2 depicts IR data for a typical transformation of an unsaturated ADMET polymer to saturated model polymer in the series studied here. The 967–969 cm^{-1} absorption in the unsaturated polymer, which corresponds to the out-of-plane C–H bend in the alkene, completely disappears after successful hydrogenation.

Further purification of the saturated polymers was accomplished via dissolution in xylene followed by precipitation in acidic methanol, repeating this procedure if necessary, until the polymers were white. The polymers seem to purify more

(21) (a) Trzaska, S. T.; Lee, L. W.; Register, R. A. *Macromolecules* **2000**, *33*, 9215–9221. (b) Singha, N. K.; De, P. P.; Sivaram, S. *J. Appl. Polym. Sci.* **1997**, *66*, 1647–1652. (c) Doi, Y.; Yano, A.; Soga, K.; Burfield, D. R. *Macromolecules* **1986**, *19*, 2409–2412.

Table 1. Molecular Weight Data for Unsaturated and Saturated ADMET Polymers

EP model polymers	methyls/1000 total carbons ^a	unsaturated copolymers versus PS ^b		saturated copolymers versus PS ^d		saturated copolymers versus EP ^e		saturated copolymers LALLS ^f	
		$M_w \times 10^{-3}$	PDI ^g	$M_w \times 10^{-3}$	PDI ^g	$M_w \times 10^{-3}$	PDI ^g	$M_w \times 10^{-3}$	PDI ^g
PE-OCTH	0	27.6	1.8	34.4	1.6	14.5	1.5	16.2	1.6
PE-1.5H	1.5	30.1	1.9	37.2	1.6	15.6	1.6	15.3	1.6
PE-7.1H	7.1	35.0	1.8	41.8	1.7	17.6	1.7	23.2	1.9
PE-13.6H	13.6	57.5	2.0	58.3	1.7	24.6	1.7	26.2	1.6
PE-25.0H	25.0	60.2	2.4	56.5	1.9	24.7	1.9	27.0	1.8
PE-43.3H	43.3	69.4	1.8	62.9	2.0	27.3	2.0	30.5	1.4
PE-55.6H	55.6	26.1	1.7	29.0	2.2	12.9	2.1	13.7	1.5
PE-97.4H	97.4 ^h	45.6	2.0	34.4	1.6	10.6	1.9	15.7	2.1

^a Determined by an average of both the ¹H NMR (300 MHz) and ¹³C NMR (125 MHz) data. ^b Molecular weight data taken using tetrahydrofuran (35 °C) relative to polystyrene standards. ^c Polydispersity index (M_w/M_n). ^d Molecular weight data taken using using trichlorobenzene at 135 °C relative to polystyrene standards. ^e Molecular weight data taken using using trichlorobenzene at 135 °C relative to an EP calibration curve using the appropriate Mark–Houwink equation. ^f Molecular weight data taken using LALLS and trichlorobenzene at 135 °C. ^g The theoretical branch content for homopolymer PE–97.4H is 100 Me/1000 total C, or 111 Me per 1000 backbone C.

Table 2. NMR Data and Branching Content of ADMET EP Copolymers

EP polymer	PE-1.5H	PE-7.1H	PE-13.6H	PE-25.0H	PE-43.3H	PE-55.6H	PE-97.4H
calculated mol % 1 ^a	2	5	10	20	40	50	100
mol % 1 by NMR ^c	1.2	5.8	11.2	21.1	38.0	50.2	97.0
mol % ethylene ^{b,e}	99.69	98.57	97.24	94.86	90.94	88.21	78.31
wt % ethylene	99.54	97.85	95.91	92.48	86.98	83.27	70.66
mol % propylene ^{c,e}	0.31	1.13	2.76	5.13	9.06	11.80	21.63
wt % propylene	0.46	2.15	4.08	7.52	13.02	16.73	29.33
Me branching ^{d,e}	1.5	7.1	13.6	25.0	43.3	55.6	97.4

^a The molar percent of 6-methyl-1,10-undecadiene added to the polymerization flask. ^b The equivalent molar percent of ethylene in a EP copolymer produced by addition polymerization. ^c The equivalent molar percent of propylene in an EP copolymer produced by addition polymerization. ^d 1B, Methyl branches/1000 total carbons. ^e Determined by averaging the ¹H and ¹³C NMR data.

easily and effectively if the saturated polymers were precipitated in warm acidic methanol (40 °C) using a blender to agitate the solution.

Molecular Weight and Branching Analysis of ADMET Polymers. Prior work in our group has shown that the weight-average molecular weight of ADMET polyethylene M_w s must exceed 24 000 g/mol versus polystyrene (PS) standards before a constant melting behavior is observed;^{18,19} consequently, measuring the molecular weight of the polymers prepared in this study is essential. The molecular weight data before and after hydrogenation for the precipitated polymers is summarized in Table 1.

The GPC data (Table 1) for the unsaturated polymers was compiled using simple differential refractive index (DRI) calibration with polystyrene standards. The M_w s for all polymers range from 29 000–63 000 g/mol (versus PS standards) and exhibit a polydispersity index (PDI) in the range of 2.0, which is sufficient for modeling conventional PE materials. Variance in molecular weight can be attributed to differences in solubility of the polymers as they form, as well as to catalyst decomposition.

The saturated EP copolymers were analyzed by three molecular weight determination methods consisting of an internal differential refractive index detector (DRI), a Viscotek differential viscosity detector (DP), and a Precision light scattering detector (LS). Using these three detectors in series the molecular weights were determined using the universal calibration method (a plot of log intrinsic viscosity $[\eta] \times$ molecular weight vs retention time) calibrated using polystyrene (PS), a universal calibration by converting the PS calibration curve to an EP calibration curve using the Mark–Houwink equation, and low-angle laser light scattering (LALLS), respectively, and the results

are shown in Table 1. The universal calibration data (second column in Table 1) was generated by calibrating the retention times using 17 Polymer Laboratory EZ-Cal polystyrene standards.

The EP calibration curve (third column in Table 1) was produced by converting the PS calibration curve to the corresponding EP curve using the appropriate Mark–Houwink equation where the intrinsic viscosity and Mark–Houwink constant (K) are related to EP copolymers using eqs 1 and 2 shown in the Experimental Section. The data derived using this method should be a better determination of the polymers actually molecular weight. However, low-angle laser light scattering was done to obtain the polymers “true” weight-average molecular weight. The variances in the molecular weights between saturated and unsaturated copolymers (Table 1) are a direct result of these different methods of data collection. We have looked at the effects on molecular weight caused by hydrogenation when going from unsaturated to saturated polymers and concluded that molecular weights are not affected by the hydrogenation process.^{18,19} All GPC traces were essentially unimodal demonstrating that copolymers are formed rather than mixtures of homopolymers. A more detailed study of these EP model copolymers, discussed here, is underway using triple detection methods (laser light scattering and viscometry) to gather data on the branching, branching uniformity, and dilute solution behavior.

Carbon and proton NMR data are presented in Table 2. The proton spectra were acquired with 160 co-added transients and used to determine the molar content of monomer **1** and branch content of the polymer. The proton NMR spectra are dominated by the sharp singlet from the linear backbone methylenes at δ 1.34 ppm. Methyl signals are observed for the branch methyls,

1B₁, (doublet centered at δ 0.915 ppm, with a J_{HH} coupling to the backbone methine of 6.4 Hz), and chain end methyls, 1s, (triplet at δ 0.945 ppm, with a J_{HH} of 6.3 Hz). Deconvolution of these overlapping resonances with an 85% Lorentzian/15% Gaussian line shape allowed segregation of signal intensity into contributions from methyl branches (6-methyl-1,10-undecadiene) and chain ends (6-methyl-1,10-undecadiene and 1,9-decadiene.) The branch content was determined by dividing the multiplicity-corrected integral of the 1B₁ methyl signal (derived from the deconvolution) into the sum of this value and the multiplicity-corrected methylene/methine integral.

The molar composition values were calculated as follows. The number of monomer **1** repeat units in the polymer were measured from the multiplicity-corrected 1B₁ methyl integral. After correction for methylene/methine contributions from monomer **1**, the remainder of the aliphatic integral was assigned to 1,9-decadiene.

Semiquantitative ¹³C NMR spectra were acquired using 4000 coadded transients, and allowing a 20 s recycle delay. Monomer **1** content was determined by integrating not only the resonance of the branch methyl (δ 20.1) but also the carbons alpha (δ 37.5) and beta (δ 27.5) to the branch point and using the average to determine the comonomer content. Because the carbon resonances close to the branch point are easily distinguished, the calculation is somewhat more facile when compared to the ¹H data. Subtracting the average branched monomer count from the rest of the carbon backbone gave the average monomer count that originated from 1,9-decadiene. For both proton and carbon NMR, the mole percent of **1** can be calculated by dividing the branch monomer count by the total monomer count arising from both **1** and **2**, which is given in Table 2 as mol % by NMR.

Summarized in Table 2 are the corresponding ethylene and propylene contents calculated as if these systems had been produced by chain-addition (insertion-type) mechanism. The data given in Table 2 is an average of values obtained by ¹H and ¹³C NMR. The calculation assumes that four moles of ethylene originate from the 1,9-decadiene repeat unit after hydrogenation of the ADMET polymer. It also assumes that an average of 3.5 moles of ethylene and 1 mole of propylene originate from the 6-methyl-1,10-undecadiene repeat unit after hydrogenation. Multiplying these values by the mole percent of each monomer, respectively, will generate the hypothetical mole percentages of ethylene and propylene. The monomer weight percentages were calculated for use in GPC-LALLS and in-line viscometry analysis.

Carbon NMR was also used to determine the exact nature of the endgroups associated with these ADMET EP copolymers. Figure 3a shows the carbon spectrum for **PE-OCTH** (hydrogenated polyoctenamer) produced using Schrock's metathesis catalyst, a spectrum which unequivocally shows that the endgroups produced after hydrogenation by this type of metathesis (ADMET) polymerization are methyls. This fact is vital when modeling polyethylene, as well as scientifically important because endgroups previously have never been observed in a hydrogenated ADMET high polymer. In the past, instrument limitations precluded spectroscopic determination of chain-end methyls (after hydrogenation). In this study, the high magnetic field and number of coadded transients (>4000) allowed us to make this observation for the first time.

Throughout the catalyst mediated ADMET cycle, high polymer is produced through the coupling of two terminal dienes (on separate monomer units) via a 2 + 2/retro 2 + 2 cycloaddition reaction. The coupling of the monomer units produces vinyl (H₂C=CH-Polymer-CH=CH₂) endgroups, giving methyl endgroups when hydrogenated. It is also possible to distinguish the two different endgroups produced during the ADMET copolymerization of 6-methyl-1,10-undecadiene (**1**) with 1,9 decadiene (**2**). These differences arise from the use of two structurally different comonomers, causing different local environments at the chain end. Termination of the copolymer by 1,9 decadiene produces endgroups (after hydrogenation) equivalent to the homopolymer **PE-OCTH**. Figure 3a shows six distinct resonances for hydrogenated poly(octenamer), 14.22 (1s), 22.91 (2s), 32.23 (3s), 29.59 (4s), 29.68 (5s), and 29.99 for the PE backbone.

Because ADMET copolymerization is random, the resulting copolymer contains endgroups from 6-methyl-1,10-undecadiene (**1**). The effect this methyl branch has on the endgroups can only be seen when examining the 4s and 3s carbons, or the carbons beta and gamma to the branch point. The methyl branch point shifts the 4s (upfield) and 3s (downfield) carbons with respect to the endgroups produced by **PE-OCTH**. The resonances produced by the chain-end carbons of 6-methyl-1,10-undecadiene are 14.22 (1s), 22.91 (2s), 32.60 (3s), 27.04 (4s), and 37.57 for the methylene alpha to the branch point (Figure 3c). Additionally, Figure 3 shows that both the 1s and 2s carbons of the chain-end are indistinguishable for both monomers; therefore, both resonances overlap in the copolymer. The equivalent carbon chemical shifts in solution for two possible chain ends suggests that the methyl branch in the copolymer affects carbons no greater than three positions from an individual branch located on the polymer backbone.

B. Thermal Analysis and Behavior. Differential scanning calorimetry was performed using a Perkin-Elmer DSC-7 equipped with Pyris software, with calibration accomplished using indium and *n*-octane as standards for all thermal transitions. Heats of fusions were referenced to indium. To erase thermal and crystallization history, samples were taken through several heating/cooling cycles with data collected on the third cycle in the series. Prior to cooling, the sample was held above the peak melting temperature, usually 10 °C, for five minutes and cooling was achieved at 10 °C/min until reaching -80 °C. The melting profile was then taken at the represented ranges shown in the figures. The DSC technique was chosen as the principal mode to examine of the morphology and structure for random methyl branched ADMET EP random copolymers. Numerous literature studies are available concerning the structure and thermal properties of branched PE (LDPE and HDPE), particularly for ethylene/propylene (EP) copolymers made by chain-addition chemistry.²⁻¹⁷ The unsaturated polymers were also examined to better understand the melting behavior and crystallization kinetic trends observed for the saturated counterparts.

A wide range of initiation procedures can be used to produce EP copolymers made by chain-addition chemistry; consequently, the branch identity, branch content, and branch homogeneity of these polymers differ considerably. These differences, which are direct results from chain transfer or chain walking mechanisms, give rise to variances in thermal properties that affect the use and processing of these polymers. Whereas, the model

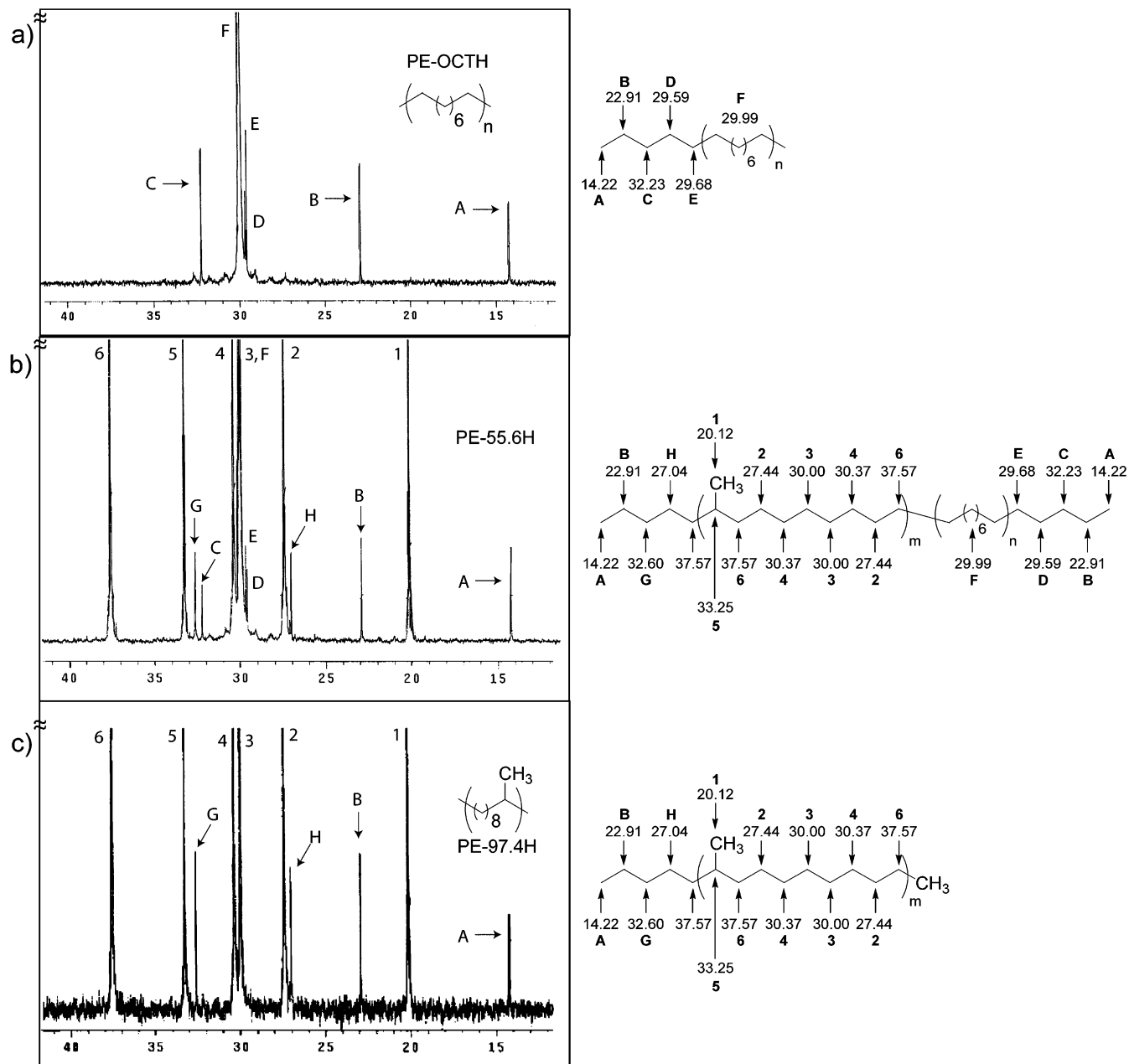


Figure 3. (a) ^{13}C NMR of unbranched PE-OCTH, (b) PE-55.6H, and (c) precisely methyl branched PE-97.4H (methyl on every 9th carbon).

ADMET EP copolymers reported herein contain a single, known branch identity (methyl), which is determined by the initial monomer's identity, a priori. The thermal behavior of the model EP polymers is summarized in Table 3. This study is focused on random methyl branched defects in PE; therefore, **PE-97.4** and **PE-97.4H**, described earlier,¹⁹ containing precise methyl branch placement are not discussed in Table 3 or the thermal behavior section.

The melting temperatures for model ADMET EP copolymers follow a similar trend found for branched commercial materials. As the methyl branch (defect) content increases, the melting point, percent crystallinity, and heat of fusion decrease. The relationship between defect content and thermal behavior is well-known and has been studied in great detail by Flory,²² Eby,²³

and Mandelkern.^{4,5} The DSC thermographs for the unsaturated and saturated versions of the first three polymers in the series are given in Figures 4 (unsaturated) and 5 (saturated) along with the traces for the unsubstituted homopolymer **PE-OCT/PE-OCTH**. The polymers exhibit both a sharp primary melting peak as well as a broad, diffuse secondary endothermic region. This secondary area, commonly referred to as the premelting region, is thought to be a regime in which quantities of smaller crystallites are melting, recrystallizing, and remelting prior to the onset of the primary melting peak.

The second set of data in the series is provided in Figure 6 (unsaturated) and Figure 7 (saturated). The polymers with the highest methyl branch content (**PE-43.3H** and **PE-55.6H**) have no distinct melting point (T_m); however, they do manifest DSC

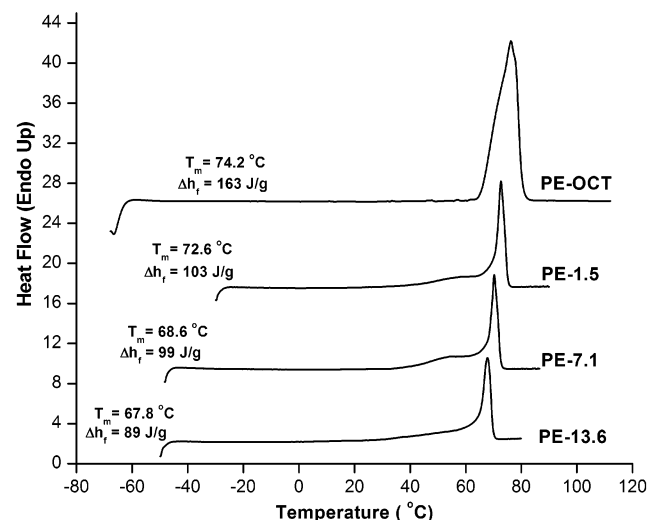
(22) Flory, P. J. *Trans. Faraday Soc.* **1955**, *51*, 848–857.

(23) Sanchez, I. C.; Eby, R. K. *J. Research Nat. B. Stand.* **1973**, *77A*, 353–358.

Table 3. Thermal Behavior of ADMET Model Copolymers

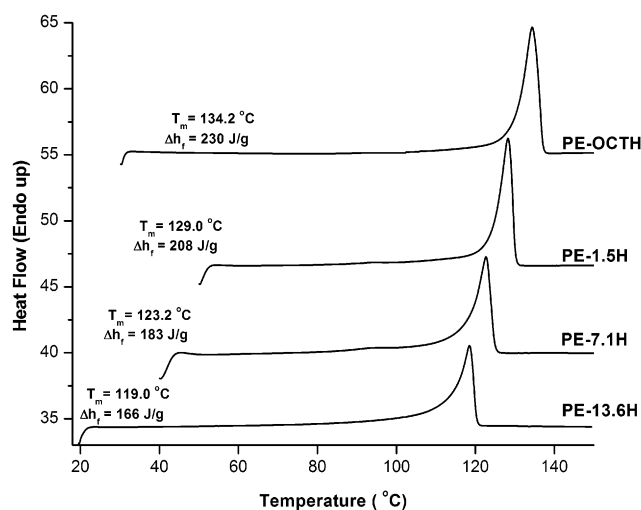
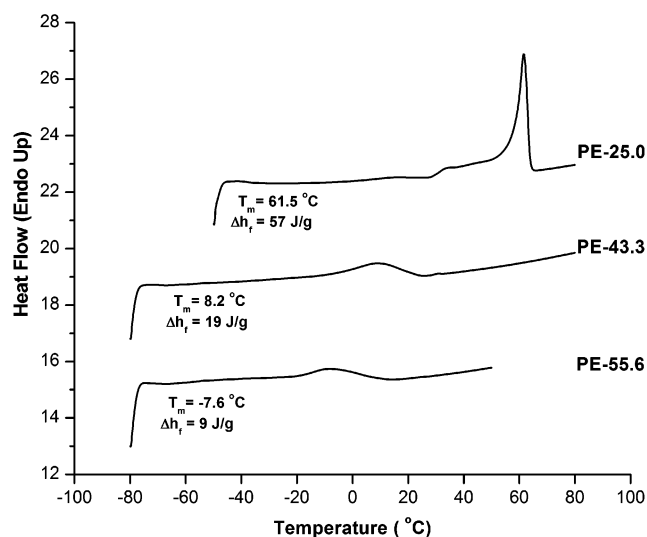
ADMET polymers (hydrogenated)	methyl branches per 1000 total carbons ^a	T_m (°C) Peak ^b	Δh_f (J/g) ^b	% crystallinity ^c
PE-OCTH	0	133.0	230.0	0.785
PE-1.5H	1.5	129.0	207.6	0.713
PE-7.1H	7.1	123.2	183.4	0.621
PE-13.6H	13.6	119.0	165.8	0.563
PE-25.0H	25.0	111.6	137.3	0.476
PE-43.3H	43.3	80.7	85.0	0.296
PE-55.6H	55.6	52.1	87.0	0.290
(unsaturated)				
PE-OCT	0	74.2	163.0	
PE-1.5	1.5	72.6	103.0	
PE-7.1	7.1	68.6	98.7	
PE-13.6	13.6	67.8	88.7	
PE-25.0	25.0	61.5	57.1	
PE-43.3	43.3	8.2	18.7	
PE-55.6	55.6	-7.6	9.0	

^a Branch content determined by averaging the ¹H (300 MHz) and ¹³C NMR (125 MHz) branch data. The branch content of unsaturated polymers is assumed to be equivalent to the saturated EP polymers. ^b Scan rate of 10 °C/min used to obtain data. ^c Percent crystallinity determined by dividing the heat of fusion by 293 J/g.²⁴

**Figure 4.** DSC Endothermic Traces for PE-OCT, PE-1.5, PE-7.1, and PE-13.6 [Scan rate = 10 °C/min].

endotherms with relatively the same low heat of fusion values. Similar behavior has been observed for ethylene-*co*-propylene polymers made by chain techniques with higher propylene content.^{3,5,15b} For example, random copolymers made using Ziegler-Natta catalysis with greater than 15% propylene incorporation generate the same type of broad, indistinct thermal curves shown here.^{3,5} However, the model EP copolymers produced by ADMET exhibit this broad, indistinct melting at lower branch density than Ziegler-Natta produced polymers, around 10–13 wt % propylene. Unsaturated copolymers **PE-43.3H** and **PE-55.6H** greatly decrease their percent crystallinity upon moderate incorporation of methyl branching. These two materials with subambient melting points, are viscous liquids at room temperature.

Several interesting results are observed in the melting behavior of the EP copolymers with randomly situated methyl branches, compared to EP model copolymers containing precisely placed branch defects reported earlier.¹⁹ In our previous study, sharp, well-defined distinct melting temperatures were observed for polymers with moderate to high branch content

**Figure 5.** DSC Endothermic Traces for PE-OCTH, PE-1.5H, PE-7.1H, and PE-13.6H [Scan rate = 10 °C/min].**Figure 6.** DSC Endothermic Traces for PE-25.0, PE-43.3, and PE-55.6 [Scan rate = 10 °C/min].

(48–111 methyls/1000 backbone carbons). Figure 8 shows **PE-45PH** ("P" stands for precise branch placement) contains methyl branches on every 21st carbon along the polymer backbone which corresponds to a branch density of 45 methyls/1000 total carbons (or 48 methyls per 1000 backbone carbons). The precisely branched EP model materials exhibit a higher order in regards to their packing ability, as compared to either the ADMET randomly branched copolymers or the PEs made by chain addition with equivalent levels of methyl branch content (Figure 8).

No distinct melting point was observed for the randomly branched **PE-43.3H** copolymer model made by metathesis chemistry (Figure 8). With respect to SCBD, Figure 8 demonstrates how important the uniformity of branch dispersion is in determining the final material's response. The sharp, well-defined endotherm generated by the precisely branched material¹⁹ is a striking result when compared to its randomly branched counterpart studied here. Evidently, the well-controlled SCBD has invoked a special crystal ordering never before observed in randomly branched PEs within the regime of comonomer content(s) studied here.

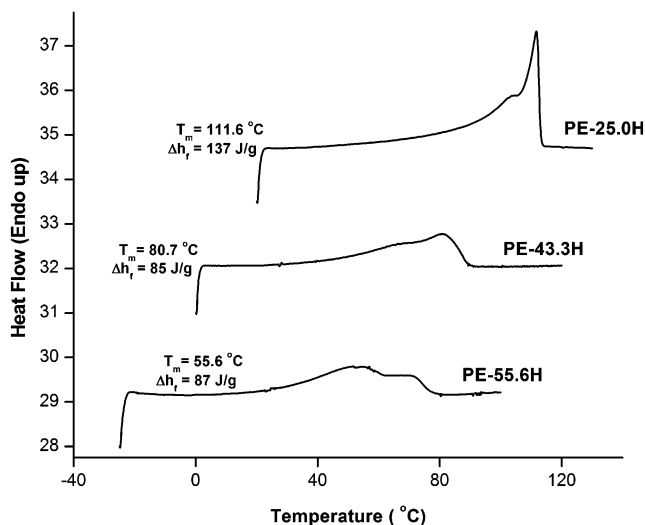


Figure 7. DSC Endothermic Traces for PE-25.0 H, PE-43.3H, and PE-55.6H [Scan rate = 10 °C/min].

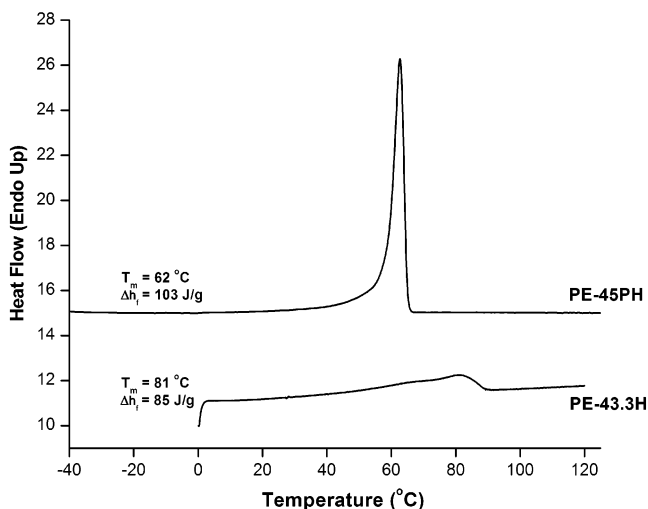


Figure 8. Thermal Comparison of Random (PE-43.3H) Versus Precise Methyl Branching (PE-45PH) [Scan rate = 10 °C/min].

The thermal behavior of the randomly branched ADMET polymers illustrates a dependence on the branch content or methyl comonomer composition. Plotting the branch content of these polymers versus their respective peak T_m 's (in Kelvin), an approach similar to the Flory equation,²² corresponds to an unbranched PE having a $T_m = 134$ °C (Figure 9a). ADMET PE produced by the hydrogenation of poly(octenamer) exhibits the same peak melting temperature (134 °C), within the T_m range of commercially produced HDPE (134–138 °C). Further, a comparison was made to Flory's infinite molecular weight linear polyethylenes by plotting percent crystallinity versus peak melting temperature (T_m). In this case, percent crystallinity was calculated using DSC techniques by dividing the heats of fusion obtained for each model polymer by 293 J/g.²⁴ The percent crystallinities are provided in Table 3. The data, when plotted in this fashion, illustrates that the ADMET polymers agree with the commonly accepted observations by Flory, Wunderlich, and Mandelkern, which demonstrates that unbranched ultrahigh molecular weight PE should have a $T_m = 141.5$ – 145.5

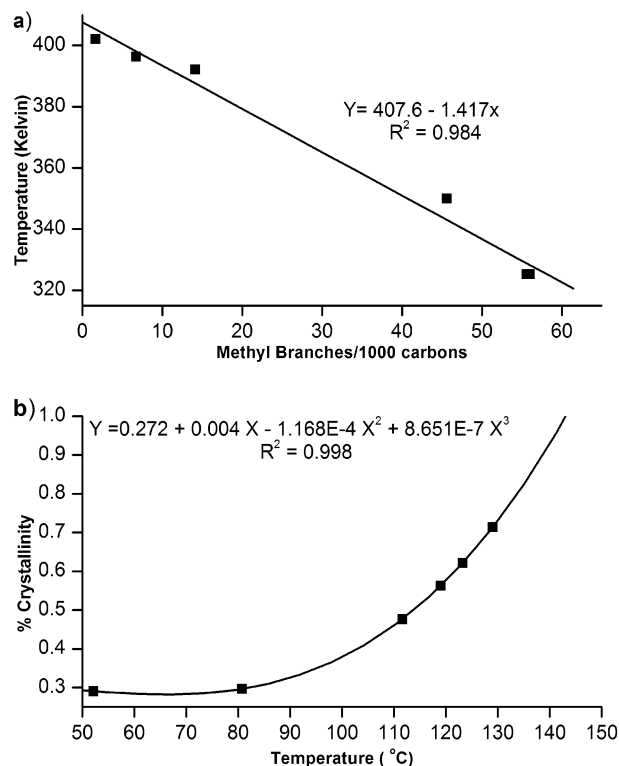


Figure 9. (a) Plot of Melting Temperature vs Methyl Branching and b) Plot of Percent Crystallinity vs Melting Temperature [Scan rate = 10 °C/min].

^{°C.22,24,25} The data provided by these ADMET PEs lead to the conclusion that perfectly linear, chain extended ADMET PE should have a $T_m = 143.5$ °C (at a 10 °C/min scan rate), when using Wunderlich's heat of fusion data (Figure 9b). Extrapolation to the samples' equilibrium melting temperature (scan rate = 0 °C/min) to avoid superheating was not performed in this initial study.

C. IR and Diffraction Data. In addition to using DSC and NMR to characterize ADMET model PE and EP copolymers, we have examined the crystal structure of our ADMET EP systems via infrared spectroscopy. The IR absorbance spectra are given in Figure 10 for a sampling of the random EP ADMET copolymers synthesized in this study. Previously, Tashiro et al. conducted a detailed study concerning polyethylene crystal structures and their corresponding IR absorbances. They concluded that the scissoring at 1466 cm^{-1} and methylene rock at 721 cm^{-1} indicate a hexagonal crystal structure for linear PE, whereas the double methylene rock at 719 and 730 cm^{-1} and single band at 1471 cm^{-1} arises from the orthorhombic crystal of PE.^{11a,26} In our case, the homopolymer arising from the polymerization of 6-methyl-1,10-undecadiene (**PE-97.4H**) exhibits absorbances at 722 cm^{-1} corresponding to the CH_2 rocking of the backbone methylene groups, and a singlet scissoring absorbance at 1465 cm^{-1} indicating a hexagonal crystal, whereas ADMET PE (**PE-OCTH**) shows absorbances at 729 and 720 cm^{-1} and 1470 cm^{-1} resulting from an orthorhombic crystal. However, when comparing the copolymer series, as the molar ratio of 6-methyl-1,10-undecadiene in-

(24) Wunderlich, B. *The Defect Crystal*. *Macromolecular Physics*, 1, Academic Press Inc.: New York, 1973; Vol. 1, 401–407.

(25) Mandelkern, L. *Crystallization of Polymers*; McGraw-Hill: New York, 1963; 1–519.

(26) Tashiro, K.; Sasaki, S.; Kobayashi, M. *Macromolecules* **1996**, *29*, 7460–7469.

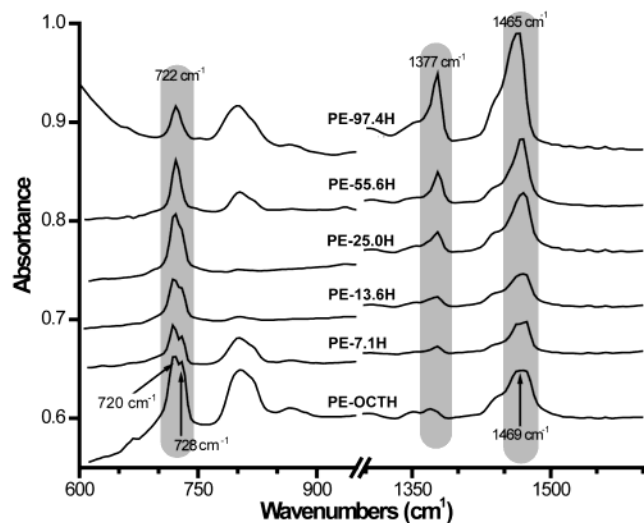


Figure 10. IR Spectral Changes with increased branch content.

creases, the absorbance characteristics approach and eventually convert to those exhibited for **PE-97.4H**. This can be seen by the transformation from a double to a single absorbance peak in the CH_2 rocking region ($720\text{--}728\text{ cm}^{-1}$ region) in going from **PE-OCTH** to **PE-97.4H**. The sharp peak at 1377 cm^{-1} (Figure 10) corresponds to the symmetrical methyl bend, which increases in relative absorbance as the methyl branch content increases.

The behavior observed for the polymers throughout this study supports the conclusions made by Tashiro.²⁶ The absorbances seen at 722 and 1465 cm^{-1} correspond to a hexagonal crystal structure, which correlate to findings for EP model materials with precise methyl branching¹⁹ as determined by electron diffraction.²⁷ ADMET PE shows orthorhombic nature when compared to Tashiro's observations and an orthorhombic–hexagonal crystal transition is seen with moderate incorporation of methyl branches (defects). To further substantiate these IR findings, wide-angle X-ray diffraction (WAXD) was performed on the series of copolymers to demonstrate that the absence of Davidov splitting in the methylene rocking and bending modes is a result of a hexagonal phase, and not the result of a highly distorted orthorhombic crystal (Figure 11).

Inspection of Figure 11 provides substantial proof for the formation of a new crystalline phase in these ADMET polyethylenes when the number of statistically placed methyl branches is increased. **PE-OCTH** produced two main intensities at d -spacings of 4.11 and 3.70 \AA (Figure 11a). Respectively, these maxima correspond precisely with the normally observed, characteristic 110 and 200 reflections for the orthorhombic unit cell of high-density polyethylene (HDPE).^{28,29} This result is in agreement with what is expected for a defect-free ethylene-based material. However, as illustrated in Figure 11b, the diffraction pattern changes substantially for the ADMET EP copolymer containing 55.6 methyl branches per 1000 carbons (**PE-55.6H**). Noteworthy differences become evident when comparing Figure 11a (**PE-OCTH**) to Figure 11b (**PE-55.6H**).

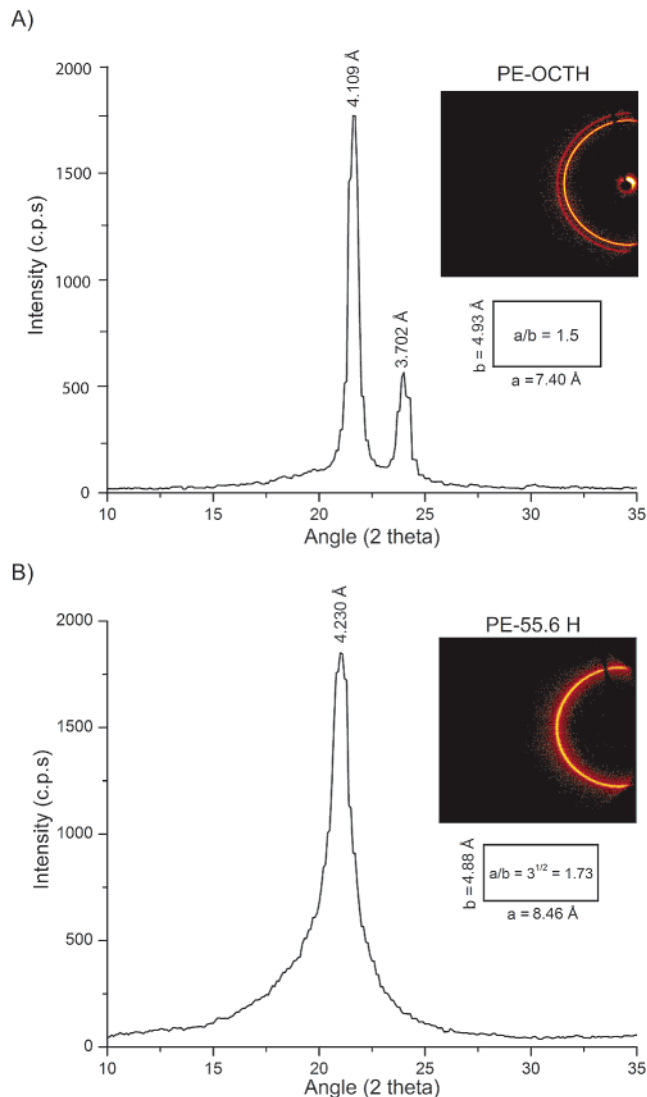


Figure 11. WAXD of (a) ADMET polyethylene (**PE-OCTH**) and (b) **PE-55.6H**. The figure shows the a and b dimensions of the unit cell (referred to orthohexagonal axes for **PE-55.6H**) and the a/b unit cell parameter.

First, Figure 11b shows only one intense peak for the ADMET EP copolymer (**PE-55.6H**) with a d -spacing of 4.23 \AA —this differs substantially from the diffractogram of **PE-OCTH** (Figure 11a), which contains two clear maxima. Second, the Bragg reflection for the 110 peak (4.11 \AA) for **PE-OCTH** shifts to 4.23 \AA in Figure 11b. In fact, in **PE-OCTH** there is no existence of the 200 reflection observed in Figure 11a. The peak also increases in its relative intensity and broadens as is evident by comparison to the 110 reflection obtained in the WAXD of **PE-OCTH** (Figure 11a). These results point to the presence of another crystallite form; indeed, the d -spacing of 4.23 \AA is not predicted for the orthorhombic form and could possibly originate from three known structures of PE: (a) monoclinic,³⁰ (b) triclinic,³¹ or (c) hexagonal.²⁸ The most likely explanation is that the d -spacing observed at 4.23 \AA (Figure 11b) arises from the reflection of the 100 Bragg plane in the hexagonal phase of polyethylene.²⁸ Moreover, simple division of the unit cell parameter a by b deduces the a/b ratio for **PE-**

(27) Manuscript in preparation.

(28) (a) Bassett, D. C.; Block, S.; Piermarini, G. J. *J. Appl. Phys.* **1974**, *45*(10), 4146–4150. (b) Yasuniwa, M.; Enoshita, R.; Takemura, T. *Jpn. J. Appl. Phys.* **1976**, *15*(8), 1421–1428. (c) Yamamoto, T.; Miyaji, H.; Asai, K. *Jpn. J. Appl. Phys.* **1977**, *16*(11), 1891–1898. (d) Rastogi, S.; Kurelec, L.; Lemstra, P. J. *Macromolecules* **1998**, *31*, 5022–5031.

(29) Bunn, W. C. *Trans. Faraday* **1939**, *35*, 482–491.

(30) Seto, T.; Hara, T.; Tanaka, K. *Jpn. J. Appl. Phys.* **1968**, *7*, 31–42.

(31) (a) Turner-Jones, A. *J. Polym. Sci.* **1962**, *62*(174), s53–56. (b) Teare, P. W.; Holmes, D. R. *J. Polym. Sci.* **1957**, *24*, 496–499. (c) Müller, A.; Lonsdale, K. *Acta Crystallogr.* **1948**, *1*, 129–131.

55.6H equaling $3^{1/2}$, which is the expected value for a hexagonal crystal (see inset, Figure 11b).

The hexagonal phase found in paraffinoid substances and in some cases polyethylene primarily is caused by chemical defects within the crystal. In fact, the hexagonal phase in PE has been observed previously at room temperature in irradiated (gamma or electron energy) samples and in copolymers containing small diene components.³² The effect on the polymers crystal lattice in both cases is the same. The observed changes are brought about by defects produced by main chain scission, double bond formation, or cross-linking.³² This disordered phase can also be produced in highly extended fibers, albeit at higher temperatures³³ or under high hydrostatic pressure.²⁸ We are able to force this hexagonal change at room temperature in our ADMET copolymers by the addition of randomized branch defects which in this case are only methyl groups. In cases where lattice defects are produced (irradiation, diene addition, and randomized methyl branches), the orthorhombic–hexagonal transition decreases below the polymers observed T_m allowing for its observability. Therefore, varying the branch content in these ADMET EP systems represents the first example of an orthorhombic-to-hexagonal phase transition in an ethylene-based copolymer without any previous external manipulation of the material (i.e., high temperature, high pressure, irradiation, etc.).

Conclusions

Acyclic diene metathesis (ADMET) polymerization has proven useful in modeling random ethylene/ α -olefin copolymers. In these EP random copolymers, as the weight percent propylene is increased, both the melting points and the heats of fusion decrease. Therefore, the thermal behavior of the methyl branched random copolymers correlates well to Flory's and Wunderlich's observations based on linear chain extended PE. By using this methodology, the theoretical melting point (T_m) for ADMET PE was found to be 143.5 °C (at a 10 °C/min scan rate) by extrapolation.

Copolymers produced via ADMET polymerization have shown properties unique in both their thermal behavior and morphology. These random EP copolymers show the ability to change conformation in crystal packing/arrangement, depending on propylene content. On incorporation of approximately 10 mol % propylene, a switch from an orthorhombic to a hexagonal crystal arrangement can be observed by IR spectroscopy and WAXD. This is the first example of conformational switching to the hexagonal phase in ethylene/propylene copolymers containing moderate methyl branch (defect) content without external sample manipulation prior to analysis. A more detailed study of this conformational switching in ADMET EP copolymers is in progress.

The exact nature of the endgroups produced by ADMET polymerization has been observed for the first time by carbon NMR. The methyl endgroups produced after hydrogenation must originate from vinyl endgroups, which are produced throughout the ADMET polymerization cycle. Therefore, these model EP

copolymers and all hydrogenated polymers produced by ADMET chemistry contain methyl endgroups— independent of monomer type and polymerization conditions. It is possible to distinguish between the two different endgroups produced in an ADMET random copolymerization.

We are continuing this research by gathering X-ray diffraction data to better understand the differences between random and precise branching in ethylene/propylene model copolymers. In addition, we are currently expanding our study of short chain branching in PE to ethyl, butyl, and hexyl branches incorporated in both a precise and a random arrangement.

Experimental Section

1.1. Instrumentation and Analysis. All ^1H NMR (300 MHz) and ^{13}C NMR (75 MHz) spectra of the unsaturated ADMET polymers were recorded on either a Varian Associates Gemini 300 or a Varian Associates Mercury 300 spectrometer. Chemical shifts for ^1H and ^{13}C NMR data were referenced to residual signals from CDCl_3 (7.23 for ^1H and 77.23 for ^{13}C) with 0.03% v/v TMS as an internal reference.

The saturated ethylene/propylene model copolymers were prepared for NMR spectroscopic analysis by dissolution in tetrachloroethane- d_2 as an approximately 5 weight-% solution. Sample preparation and data acquisition were performed at a temperature of 120 °C. Proton NMR spectra were acquired on a Varian Unity INOVA 300 spectrometer using a 5 mm switchable probe. For each ^1H spectrum, 160 transients were co-averaged using a 90-acquire pulse sequence, with a total pulse delay of 10.8 s. Spectra were Fourier transformed to 64 K complex points with line broadening of 0.2 Hz. The chemical shift scale was referenced by setting the resonance from residual tetrachloroethane protons to δ 5.98 ppm. The same samples were run for carbon NMR on a Varian UnityPlus 500, also in a 5 mm switchable probe. For each ^{13}C spectrum, 4000 transients were coaveraged, using a 90-acquire pulse sequence with full decoupling to obtain optimal nuclear Overhauser enhancement (nOe). Broadband decoupling was performed with WALTZ-16 modulation. A total pulse delay time of 20.9 s was employed. The spectra were Fourier transformed to 64 K points, with 1 Hz line broadening.

Gel permeation chromatography (GPC) of the unsaturated ADMET polymers was performed using two 300 mm Polymer Laboratories gel 5 μm mixed-C columns. The instrument consisted of a Rainin SD-300 pump, Hewlett-Packard 1047-A RI detector (254 nm), TC-45 Eppendorf column heater set to 35 °C, and Waters U6K injector. The solvent used was THF at a flow rate of 1.0 mL/min. Polymer samples were dissolved in HPLC grade THF (approximately 0.1% w/v) and filtered before injection. Retention times were calibrated to polystyrene standards from Polymer Laboratories (Amherst, MA). In all cases, peak integration has been truncated to exclude any contribution from lower molecular weight cyclic materials.

High-temperature gel permeation chromatography (HTGPC) of the saturated EP model copolymers was performed on a Waters 150C with its internal differential refractive index detector (DRI), a Viscotek differential viscosity detector (DP), and a Precision light scattering detector (LS). The light scattering signal was collected at a 15° angle, and the three in-line detectors were operated in series in the order of LS–DP–DRI. The chromatography was performed at 135 °C using three Polymer Laboratory mixed-bed type B columns (10 microns PD, 7.8 mm ID, 300 mm length) with inhibited trichlorobenzene as the mobile phase at a flow rate of 0.5 mL/minute. Injection mass for the samples varied between 0.600 and 0.750 mg using a 300 μL injection volume.

Data analysis for the high-temperature GPC was performed using an in-house program developed at ExxonMobil.²⁰ This program calculates the molecular weight distributions in two ways: (1) by triple detection (LALLS), directly from the detector signals using the Zimm

- (32) (a) Vaughan, A. S.; Unger, G.; Bassett, D. C.; Keller, A. *Polymer* **1985**, *26*, 726–732. (b) Unger, G.; Keller, A. *Polymer* **1980**, *21*, 1273–1277. (c) Unger, G. *Polymer* **1980**, *21*, 1278–1283. (d) Unger, G.; Grubb, D. T.; Keller, A. *Polymer* **1980**, *21*, 1284–1291. (e) Orth, H.; Fisher, E. W. *Makromol. Chem.* **1965**, *88*, 188–201.
- (33) (a) Kuwabara, K.; Horii, F. *Macromolecules* **1999**, *32*, 5600–5605. (b) Clough, S. B. *Polym. Lett.* **1970**, *8*, 519–523. (c) Pennings, A. J.; Zwijnenburg, A. J. *Polym. Sci. (Polym. Phys. ed.)* **1979**, *17*, 1011–1032.

equation, and (2) by DRI detector using universal calibration and the Mark–Houwink relationship.

Methodology for LALLS. Molecular weight was calculated from the LS and DRI signals. The DP detector was used to measure sample intrinsic viscosity and to examine the Mark–Houwink relationship, $\log(\text{intrinsic viscosity}) - \log(\text{molecular weight})$, to be presented in a future paper (because EP copolymers are well characterized, it was not necessary to use the intrinsic viscosity to estimate the virial coefficient, A_2 , for purposes of molecular weight calculations in this work). The inter-detector volumes were determined by shifting their values in the software to obtain the best overlap of the three normalized signals for two suitably narrow polystyrene standards. The detector response factors used to convert the raw data to polymer molecular weights were determined by running a series of polymer standards (the two polystyrene standards used to determine the inter-detector volume, three narrow, and one broad PE standards from NIST and one broad PP standard), for which the M_w , intrinsic viscosity, and injection mass are known. The DRI response factor was determined by first optimizing the agreement between the concentration calculated from the integrated peak areas and from the injection mass for the seven samples. The light scattering response factor was then determined by optimizing the agreement between the M_w values calculated for each of the narrow standards compared to the literature values. Similarly, the intrinsic viscosity response factor was calculated by optimizing the agreement between the calculated and literature values for the five narrow standards.

Methodology for high-temperature DRI detection: Retention times were calibrated using 17 Polymer Laboratory EZ-Cal polystyrene standards. For each sample, the PS calibration curve is converted to a corresponding EP calibration curve using the appropriate Mark–Houwink equation for the polymer composition. The Mark–Houwink parameters for each EP composition were calculated from PE using eq 1

$$[\eta]_{EP} = [\eta]_{PE} * (1 - 0.0053015 * \text{wt \% propylene})$$

Equation 1. Mark–Houwink equation using EP compositions.

If it is assumed that the molecular weight exponent α does not vary significantly with copolymer composition (a reasonable assumption since α for PE and PP are very similar), then this equation can be rewritten as eq 2, where wt % propylene is determined by NMR and K_{PE} is taken from the literature (eq 2)²⁰

$$K_{EP} = K_{PE} * (1 - 0.0053015 * \text{wt \% propylene})$$

Equation 2. Mark–Houwink equation using NMR-determined wt % propylene content.

Fourier transform infrared (FT-IR) spectrometry was performed using a Bio-Rad FTS-40A spectrometer. The hydrogenation of the unsaturated ADMET polymers was monitored by the disappearance of the out-of-plane bend for the trans internal double bond at 967 cm^{-1} . The samples were prepared by grinding the polymer with IR grade KBr into a homogeneous mixture and analyzed using a KBr pellet formed from the mixture.

Differential scanning calorimetry (DSC) was performed using a Perkin-Elmer DSC 7 at a heating rate of 10 $^{\circ}\text{C}/\text{min}$. Thermal calibrations were made using indium and freshly distilled *n*-octane as references for thermal transitions. Heats of fusion were referenced against indium. The samples were scanned for multiple cycles to remove recrystallization differences between samples and the results reported are of the third scan in the cycle. The results are listed in the Experimental Section and in tabular form within the text. Reported values are given as T_m (melting peak) and Δh_m (enthalpy of melting).

Wide-angle X-ray diffraction (WAXD) patterns were collected in point collimated, monochromatic Cu $K\alpha$ (1.5418 Å) radiation on a

Bruker platform goniometer. The source was a Kristalloflex 760 2.2 kW generator and long fine focus tube equipped with cross coupled Göble mirror monochromator and 200 μm point collimation. A HI-STAR area detector was mounted for data collection at 5.9 cm and referenced to corundum (alumina). Data were processed using General Area Detector Diffraction System (GADDS) program. Prior to collection of the X-ray data, the copolymer samples were solution crystallized from toluene: methanol and dried under high vacuum until constant weight was achieved. Fine shearings of the solution crystallized material were packed in a 1.0 mm thin-walled special glass powder diffraction capillary tube manufactured by Wolfgang Muller glas technik and purchased from the Charles Supper Company (Natick, MA). The data presented were collected at 30 $^{\circ}$ 2Theta and unwarped for inhomogeneous response in the flood field of the detector.

1.2. Materials. Monomer 6-methyl-1,10-undecadiene (**1**) used in this study was synthesized following literature procedures.¹⁹ Schrock's molybdenum metathesis catalyst, $[(\text{CF}_3)_2\text{CH}_2\text{CO}]_2(\text{N}-2,6-\text{C}_6\text{H}_3-i\text{-Pr}_2)\text{Mo}=\text{CHC}(\text{CH}_3)_2\text{Ph}$ was also synthesized following literature procedures.³⁴ Wilkinson's rhodium hydrogenation catalyst $\text{RhCl}(\text{PPh}_3)_3$ was purchased from Strem Chemical and used as received. Xylenes (Fisher) and 1,9-decadiene (Aldrich) were freshly distilled over Na metal using benzophenone as the indicator. Additional reagents were used as received.

2. ADMET Copolymerizations of 1,9-Decadiene and 6-Methyl-1,10-undecadiene. General Conditions for All Polymerization Shown. All glassware was thoroughly cleaned, oven-dried, and finally flame-dried under vacuum prior to use. The monomers were dried over a potassium mirror, vacuum transferred into a Schlenk flask, and subsequently degassed (3X) prior to storage in an argon-filled drybox. Monomers were weighed based on the needed molar ratios, (X:Y) shown below, of the resulting ethylene/propylene copolymers. All metathesis reactions were initiated in the bulk, inside the drybox using 50 mL round-bottom flasks equipped with a Teflon stirbar. The flasks were then fitted with a Teflon vacuum valve, brought out of the drybox, and placed on a high vacuum line ($<10^{-3}$ mmHg) while being vigorously stirred. The polymerization vessel was exposed to intermittent vacuum at room temperature until the reaction either became highly viscous or solid (stirring ceased). The flask was then placed in a 40 $^{\circ}\text{C}$ oil bath at high vacuum ($<10^{-3}$ mmHg) for 48 h upon which the temperature was raised to 50 $^{\circ}\text{C}$ for an additional 48 h. The polymerization vessel was cooled to room temperature, and finally, the unsaturated polymer was taken up into toluene and precipitated into cold acidic methanol (1 M HCl) to remove catalyst residue. The ADMET unsaturated polymers were then fully characterized and subsequently hydrogenated.

2.1. Synthesis and Characterization of PE–55.6. Polymerization of (50:50) 6-Methyl-1,10-undecadiene (1**) and 1,9-decadiene (**2**).** Monomer **1**, 0.960 g (5.78 mmol) and **2** 0.800 g (5.78 mmol) were combined and stirred for 3 h to produce a homogeneous mixture. To this mixture was added 0.009 g (1.095×10^{-2} mmol) of Schrock's molybdenum catalyst. Precipitation from methanol (-78 $^{\circ}\text{C}$), **PE–55.6** gave: Yield: 90% (after precipitation). The following spectral properties were obtained: ^1H NMR (CDCl_3) δ 0.83 (d, 1.63 H, methyl), 1.10 (br, 1.19 H), 1.32 (br, 8.0 H), 1.98 (br, 4.29 H), 5.38 (br, 2 H, internal olefin); ^{13}C NMR (CDCl_3) δ 20.0, 27.3, 27.4, 29.2, 29.8, 32.8, 33.2, 36.9, 129.9 (cis), 130.4 (trans). ^{13}C NMR integration of cis:trans peaks: 15:85. GPC data (DRI vs PS): $M_w = 26\,100$ g/mol; PDI = 1.7 (M_w/M_n). DSC results: $T_m(\text{peak}) = -7.6$ $^{\circ}\text{C}$, $\Delta h_m = 9.0$ J/g.

- (34) (a) Schrock, R. R.; Murdzek, J. S.; Bazan, G. C.; Robbins, J.; Dimare, M.; O'Regan, M. *J. Am. Chem. Soc.* **1990**, *112*, 3875–3886. (b) Bazan, G. C.; Khosravi, E.; Schrock, R. R.; Feast, W. J.; Gibson, V. C.; O'Regan, M. B.; Thomas, J. K.; Davis, W. M. *J. Am. Chem. Soc.* **1990**, *112*, 8378–8387. (c) Bazan, G. C.; Oskam, J. H.; Cho, H. N.; Park, L. Y.; Schrock, R. R. *J. Am. Chem. Soc.* **1991**, *113*, 6899–6907. (d) Fox, H. H.; Schrock, R. R. *Organometallics* **1992**, *11*, 2763–2765. (e) Feldman, J.; Murdzek, J. S.; Davis, W. M.; Schrock, R. R. *Organometallics* **1989**, *8*, 2260–2265. (f) Oskam, J. H.; Schrock, R. R. *J. Am. Chem. Soc.* **1992**, *114*, 7588–7590.

2.2. Synthesis and Characterization of PE-43.3. Polymerization of (40:60) 6-Methyl-1,10-undecadiene (1) and 1,9-decadiene (2). Synthesized as above using 0.800 g (4.82 mmol) **1**, 1.00 g (7.20 mmol) **2**, and 0.009 g (1.095×10^{-2} mmol) of Schrock's molybdenum catalyst. Precipitation from methanol (-78°C), **PE-43.3** gave: Yield: 92% (after precipitation). The following spectral properties were obtained: ^1H NMR (CDCl_3) δ 0.83 (d, 1.34 H, methyl), 1.10 (br, 1.09 H), 1.32 (br, 8.2 H), 1.98 (br, 4.3 H), 5.38 (br, 2 H, internal olefin); ^{13}C NMR (CDCl_3) δ 20.0, 27.3, 27.4, 29.2, 29.8, 32.8, 33.2, 36.9, 129.9 (cis), 130.4 (trans). ^{13}C NMR integration of cis:trans peaks: 13:87. GPC data (DRI vs PS): $M_w = 69\,400$ g/mol; PDI = 1.8 (M_w/M_n). DSC results: $T_m(\text{peak}) = 8.2^\circ\text{C}$, $\Delta h_m = 18.7$ J/g.

2.3. Synthesis and Characterization of PE-25.0. Polymerization of (20:80) 6-Methyl-1,10-undecadiene (1) and 1,9-decadiene (2). Synthesized as above using 0.432 g (2.60 mmol) **1**, 1.44 g (10.4 mmol) **2**, and 0.008 g (1.087×10^{-2} mmol) of Schrock's molybdenum catalyst. Precipitation from methanol, **PE-25.0** gave: Yield: 97% (after precipitation). The following spectral properties were obtained: ^1H NMR (CDCl_3) δ 0.83 (d, 0.70 H, methyl), 1.10 (br, 0.59 H), 1.32 (br, 8.0 H), 1.98 (br, 4.2 H), 5.38 (br, 2 H, internal olefin); ^{13}C NMR (CDCl_3) δ 20.0, 27.3, 27.4, 29.2, 29.8, 32.8, 33.2, 36.9, 129.9 (cis), 130.4 (trans). ^{13}C NMR integration of cis:trans peaks: 11:89. GPC data (DRI vs PS): $M_w = 60\,200$ g/mol; PDI = 2.4 (M_w/M_n). DSC results: $T_m(\text{peak}) = 61.5^\circ\text{C}$, $\Delta h_m = 57.1$ J/g.

2.4. Synthesis and Characterization of PE-13.6. Polymerization of (10:90) 6-Methyl-1,10-undecadiene (1) and 1,9-decadiene (2). Synthesized as above using 0.220 g (1.32 mmol) **1**, 1.70 g (12.3 mmol) **2**, and 0.009 g (1.095×10^{-2} mmol) of Schrock's molybdenum catalyst. Precipitation from methanol, **PE-13.6** gave: Yield: 97% (after precipitation). The following spectral properties were obtained: ^1H NMR (CDCl_3) δ 0.83 (d, 0.27 H, methyl), 1.10 (br, 0.23 H), 1.32 (br, 7.6 H), 1.98 (br, 4.0 H), 5.38 (br, 2 H, internal olefin); ^{13}C NMR (CDCl_3) δ 20.0, 27.3, 27.4, 29.2, 29.8, 32.8, 33.2, 36.9, 129.9 (cis), 130.4 (trans). ^{13}C NMR integration of cis:trans peaks: 9:91. GPC data (DRI vs PS): $M_w = 57\,500$ g/mol; PDI = 2.0 (M_w/M_n). DSC results: $T_m(\text{peak}) = 67.8^\circ\text{C}$, $\Delta h_m = 88.7$ J/g.

2.5. Synthesis and Characterization of PE-7.1. Polymerization of (5:95) 6-Methyl-1,10-undecadiene (1) and 1,9-decadiene (2). Synthesized as above using 0.113 g (0.681 mmol) **1**, 1.77 g (13.0 mmol) **2**, and 0.010 g (1.37×10^{-2} mmol) of Schrock's molybdenum catalyst. Precipitation from methanol, **PE-7.1** gave: Yield: 98% (after precipitation). The following spectral properties were obtained: ^1H NMR (CDCl_3) δ 0.83 (d, 0.14 H, methyl), 1.10 (br, 0.15 H), 1.32 (br, 8.13 H), 1.98 (br, 4.14 H), 5.38 (br, 2 H, internal olefin); ^{13}C NMR (CDCl_3) δ 20.0, 27.3, 27.4, 29.2, 29.8, 32.8, 33.2, 36.9, 129.9 (cis), 130.4 (trans). ^{13}C NMR integration of cis:trans peaks: 7:93. GPC data (DRI vs PS): $M_w = 35\,000$ g/mol; PDI = 1.8 (M_w/M_n). DSC results: $T_m(\text{peak}) = 68.6^\circ\text{C}$, $\Delta h_m = 98.7$ J/g.

2.6. Synthesis and Characterization of PE-1.5. Polymerization of (1:99) 6-Methyl-1,10-undecadiene (1) and 1,9-decadiene (2). Synthesized as above using 0.021 g (0.124 mmol) **1**, 1.70 g (12.3 mmol) **2**, and 0.008 g (1.087×10^{-2} mmol) of Schrock's molybdenum catalyst. Precipitation from methanol, **PE-1.5** gave: Yield: 98% (after precipitation). The following spectral properties were obtained: ^1H NMR (CDCl_3) δ 0.83 (d, 0.04 H, methyl), 1.10 (br, 0.08), 1.32 (br, 7.25 H), 1.98 (br, 4.0 H), 5.38 (br, 2 H, internal olefin); ^{13}C NMR (CDCl_3) δ 20.0, 27.3, 27.4, 29.2, 29.8, 32.8, 33.2, 36.9, 129.9 (cis), 130.4 (trans). ^{13}C NMR integration of cis:trans peaks: 4:96. GPC data (DRI vs PS): $M_w = 30\,100$ g/mol; PDI = 1.9 (M_w/M_n). DSC results: $T_m(\text{peak}) = 72.6^\circ\text{C}$, $\Delta h_m = 103.0$ J/g.

2.7. Synthesis and Characterization of PE-OCT. Polymerization of 1,9-Decadiene (2). Monomer **2**, 2.00 g (14.47 mmol), was combined with 0.011 g (1.446×10^{-2} mmol) of Schrock's molybdenum catalyst. The resulting unsaturated polymer (**PE-OCT**) was analyzed after precipitation from methanol. Yield: 98% (after precipitation). The following spectral properties were obtained: ^1H NMR (CDCl_3) δ 1.32

(br, 8.0 H), 1.98 (br, 4.0 H), 5.38 (br, 2 H, internal olefin); ^{13}C NMR (CDCl_3) δ 29.2, 29.8, 32.8, 129.9 (cis), 130.4 (trans). ^{13}C NMR integration of cis:trans peaks: 4:96. GPC data (DRI vs PS): $M_w = 27\,600$ g/mol; PDI = 1.8 (M_w/M_n). DSC results: $T_m(\text{peak}) = 74.2^\circ\text{C}$, $\Delta h_m = 163$ J/g.

3. Hydrogenation of Unsaturated ADMET Polymers. Synthesis and Characterization of PE-55.6H. Hydrogenations were performed using a 150 mL Parr high-pressure reaction vessel equipped with a glass liner and Teflon stirbar. Unsaturated polymer **PE-50** (1.00 g) and Wilkinson's catalyst (0.020 g) were added to the glass liner under a nitrogen blanket. Finally, 20 mL of xylenes were added. The vessel was sealed and attached to a grade 5 hydrogen tank and purged with hydrogen several times. The bomb was charged with 700 psi of H_2 and stirred for 96 h at 120°C . The hydrogenated polymer **PE-55.6H** was dissolved in boiling toluene, filtered, and precipitated into 40°C methanol. The polymer was then filtered and then dried under reduced pressure until a constant weight was obtained. Yield: 97% (after precipitation). The following spectral properties were obtained: ^1H NMR ($\text{TCE-}d_2$) δ 0.915 (d, CH_3 , 95 H), 1.19 and 1.34 (br, CH_2 , 1000 H). ^{13}C NMR ($\text{TCE-}d_2$) δ 14.22, 20.13 (CH_3), 22.91, 27.04, 27.44, 29.59, 29.68, 29.99, 30.00, 30.37, 32.23, 32.60, 33.25, 37.57 (CH). GPC data (LALLS): $M_w = 13\,700$ g/mol; PDI = 1.5 (M_w/M_n). DSC results: $T_m(\text{peak}) = 52.1^\circ\text{C}$, $\Delta h_m = 87.0$ J/g.

3.1. Synthesis and Characterization of PE-43.3H. Synthesized following procedure shown above. Yield: 98% (after precipitation). The following spectral properties were obtained: ^1H NMR ($\text{TCE-}d_2$) δ 0.915 (d, CH_3 , 73.1 H), 1.19 and 1.34 (br, CH_2 , 1000 H). ^{13}C NMR ($\text{TCE-}d_2$) δ 14.22, 20.13 (CH_3), 22.91, 27.04, 27.44, 29.59, 29.68, 29.99, 30.00, 30.37, 32.23, 32.60, 33.25, 37.57 (CH). GPC data (LALLS): $M_w = 30\,500$ g/mol; PDI = 1.4 (M_w/M_n). DSC results: $T_m(\text{peak}) = 80.7^\circ\text{C}$, $\Delta h_m = 85.0$ J/g.

3.2. Synthesis and Characterization of PE-25.0H. Synthesized following procedure shown above. Yield: 98% (after precipitation). The following spectral properties were obtained: ^1H NMR ($\text{TCE-}d_2$) δ 0.915 (d, CH_3 , 44.57 H), 1.19 and 1.34 (br, CH_2 , 1000 H). ^{13}C NMR ($\text{TCE-}d_2$) δ 14.22, 20.13 (CH_3), 22.91, 27.04, 27.44, 29.59, 29.68, 29.99, 30.00, 30.37, 32.23, 32.60, 33.25, 37.57 (CH). GPC data (LALLS): $M_w = 27\,000$ g/mol; PDI = 1.8 (M_w/M_n). DSC results: $T_m(\text{peak}) = 111.6^\circ\text{C}$, $\Delta h_m = 137.3$ J/g.

3.3. Synthesis and Characterization of PE-13.6H. Synthesized following procedure shown above. Yield: 99% (after precipitation). The following spectral properties were obtained: ^1H NMR ($\text{TCE-}d_2$) δ 0.915 (d, CH_3 , 38.72 H), 1.19 and 1.34 (br, CH_2 , 1000 H). ^{13}C NMR ($\text{TCE-}d_2$) δ 14.22, 20.13 (CH_3), 22.91, 27.04, 27.44, 29.59, 29.68, 29.99, 30.00, 30.37, 32.23, 32.60, 33.25, 37.57 (CH). GPC data (LALLS): $M_w = 26\,200$ g/mol; PDI = 1.6 (M_w/M_n). DSC results: $T_m(\text{peak}) = 119.0^\circ\text{C}$, $\Delta h_m = 165.8$ J/g.

3.4. Synthesis and Characterization of PE-7.1H. Synthesized following procedure shown above. Yield: 98% (after precipitation). The following spectral properties were obtained: ^1H NMR ($\text{TCE-}d_2$) δ 0.915 (d, CH_3 , 24.23 H), 1.19 and 1.34 (br, CH_2 , 1000 H). ^{13}C NMR ($\text{TCE-}d_2$) δ 14.22, 20.13 (CH_3), 22.91, 27.04, 27.44, 29.59, 29.68, 29.99, 30.00, 30.37, 32.23, 32.60, 33.25, 37.57 (CH). GPC data (LALLS): $M_w = 23\,200$ g/mol; PDI = 1.9 (M_w/M_n). DSC results: $T_m(\text{peak}) = 123.2^\circ\text{C}$, $\Delta h_m = 183.4$ J/g.

3.5. Synthesis and Characterization of PE-1.5H. Synthesized following procedure shown above. Yield: 99% (after precipitation). The following spectral properties were obtained: ^1H NMR ($\text{TCE-}d_2$) δ 0.915 (d, CH_3 , 11.72 H), 1.19 and 1.34 (br, CH_2 , 1000 H). ^{13}C NMR ($\text{TCE-}d_2$) δ 14.22, 20.13 (CH_3), 22.91, 27.04, 27.44, 29.59, 29.68, 29.99, 30.00, 30.37, 32.23, 32.60, 33.25, 37.57 (CH). GPC data (LALLS): $M_w = 15\,300$ g/mol; PDI = 1.6 (M_w/M_n). DSC results: $T_m(\text{peak}) = 129.0^\circ\text{C}$, $\Delta h_m = 207.6$ J/g.

3.6. Synthesis and Characterization of PE-OCTH. Synthesized following procedure shown above. Yield: 98% (after precipitation). The following spectral properties were obtained: ^1H NMR ($\text{TCE-}d_2$)

δ 0.915 (d, CH₃, 10.63 H), 1.19 and 1.34 (br, CH₂, 1000 H). ¹³C NMR (TCE-*d*₂) δ 14.22 (1s), 22.91 (2s), 29.59 (4s), 29.68 (5s), 29.99, 32.23 (3s). GPC data (LALLS): $M_w = 16\,200$ g/mol; PDI = 1.6 (M_w/M_n). DSC results: $T_m(\text{peak}) = 133$ °C, $\Delta h_m = 230.0$ J/g.

Acknowledgment. We wish to thank the National Science Foundation (Grant No. DMR9806492) for financial support of

this research. The authors would especially like to thank Louise M. Wheeler, Joseph Olkusz, and Mark Genowitz for the high temperature GPC/light scattering analysis, Boming Liang for his assistance obtaining NMR spectra, Andrew Skolnik and Dr. Randy Duran for his help obtaining X-ray diffraction.

JA020862V